

## PAPER

View Article Online  
View Journal | View IssueCite this: *RSC Adv.*, 2017, 7, 37844

## Photo-sensitive benzoxazine II: chalcone-containing benzoxazine and its photo and thermal-cured thermoset†

Ching Hsuan Lin, <sup>a</sup> Chun Kai Chien, <sup>a</sup> Chien Han Chen<sup>a</sup> and Tzong Yuan Juang<sup>\*b</sup>

A chalcone-containing benzoxazine (BHP-a) was synthesized from a chalcone-containing bisphenol: 1,3-bis(4-hydroxyphenyl) propanone (BHP), aniline and paraformaldehyde in a co-solvent of xylene/1-butanol (2/1, V/V). The structure of BHP-a was successfully confirmed by FTIR, <sup>1</sup>H and <sup>13</sup>C-NMR spectra. After thermal treatment at a temperature higher than 240 °C, BHP becomes insoluble. This indicates that the double bond of the chalcone moiety of BHP can be thermally polymerized at elevated temperature. The UV spectrum shows that the chalcone moiety of BHP-a underwent dimerization *via* [2π + 2π] cycloaddition. Therefore, two procedures were applied to cure BHP-a. The first one was thermal curing of chalcone and oxazine moieties of BHP-a. The second one was photo curing of the chalcone moiety, followed by thermal curing of the oxazine moiety. The thermal properties of thermosets based on the two procedures were evaluated. Thermosets of BHP-a exhibit a *T<sub>g</sub>* as high as 294 °C for curing procedure one, and 328 °C for curing procedure two. The value is much higher than that of a traditional bisphenol/aniline-based benzoxazine thermoset. We conclude that the curing of the double bond of the chalcone and photo dimerization of the chalcone contribute to the good thermal properties.

Received 22nd June 2017

Accepted 27th July 2017

DOI: 10.1039/c7ra06967g

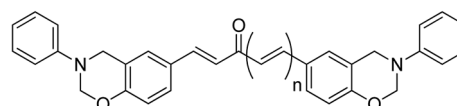
rsc.li/rsc-advances

## Introduction

Polybenzoxazines are a class of phenolic thermosets, and are generally obtained by the thermal ring-opening polymerization of benzoxazine monomers. Polybenzoxazines exhibit special characteristics such as moderate-to-high thermal properties,<sup>1–14</sup> superior membrane properties at elevated temperatures,<sup>15</sup> low shrinkage,<sup>16</sup> and low surface energy.<sup>17</sup> To further enhance their properties, studies on the curing mechanism,<sup>5,7,18–21</sup> incorporation of a multifunctional linkage<sup>22–25</sup> or photo-sensitive moieties such as methacryloyl<sup>26,27</sup> and coumarins<sup>28–30</sup> have been applied. It is known that the coumarin moiety undergoes dimerization through [2π + 2π] cycloaddition to afford a crosslinked network upon irradiation at wavelengths greater than 310 nm. Based on that chemistry, Yagci *et al.* synthesized a coumarin-containing benzoxazine, 4-methyl-9-*p*-tolyl-9,10-dihydrochromeno[8,7-*e*] [1,3]oxazin-2(8*H*)-one,<sup>28</sup> and studied the photodimerization of the coumarin moiety. Dimers of different isomers were obtained through the [2π + 2π] cyclobutane formation. Benzoxazine moieties can be polymerized through thermal ring-opening polymerization to afford highly dense crosslinked networks. Kuo *et al.* prepared a coumarin-containing

benzoxazine (coumarin-Py Bz).<sup>29,30</sup> They dimerized the coumarin-Py Bz to a dimer, the di-coumarin-Py Bz, through photodimerization of the coumarin moiety. DSC thermograms revealed that the glass transition temperature of poly(di-coumarin-Py Bz) is 227 °C, which is higher than that (200 °C) of poly(coumarin-Py Bz), a thermoset of coumarin-Py Bz without photodimerization. Yagci *et al.* prepared a series of poly(propylene oxides) bearing coumarin-benzoxazine units (PPO-Cou-Benz)s.<sup>31</sup> The coumarin moiety undergoes efficient dimerization upon irradiation at wavelengths higher than 300 nm as confirmed by UV-Vis spectral investigations. Experimental data show that it is possible to trigger self-healing in polybenzoxazine networks that are chemically bound to PPOs.

Recently, we have reported the synthesis of a bis(4-hydroxybenzylidene)acetone/aniline-based benzoxazine (BHBA-a, *n* = 1 in Scheme 1) and studied its photo- and thermally-curing behavior.<sup>32</sup> BHBA-a was photo-cured to afford a tetrafunctional benzoxazine (BHBA-a dimer), and followed by thermal curing of the double bond and oxazine linkage. The resulting thermoset shows a *T<sub>g</sub>* value as high as 342 °C was achieved.



Scheme 1 Structure of benzoxazines. The value *n* = 1 for BHBA-a (previous work),<sup>32</sup> and *n* = 0 for BHP-a (this work).

<sup>a</sup>Department of Chemical Engineering, National Chung Hsing University, Taichung, Taiwan. E-mail: linch@nchu.edu.tw

<sup>b</sup>Department of Cosmeceutics, China Medical University, Taichung, Taiwan

† Electronic supplementary information (ESI) available: Fig. S1–S5. See DOI: 10.1039/c7ra06967g

In addition to (meth)acrylate, coumarin and bisbenzylideneacetone moieties, chalcone is also a photo-sensitive moiety. It is an aromatic enone ( $\alpha,\beta$ -unsaturated carbonyl) that can be prepared by aldol condensation between a benzaldehyde and acetophenone in the presence of a base such as sodium hydroxide or  $\text{BF}_3 \cdot \text{OEt}_2$  as a catalyst.<sup>33</sup> Polymers with chalcone moiety possess photo-reactivity. For example, Feng *et al.*<sup>34</sup> and Song *et al.*<sup>35</sup> incorporated chalcone moiety into polyimides. The resulting polyimides showed photosensitivity upon light irradiation using a xenon lamp. Rehab *et al.*,<sup>36</sup> Nanjundan *et al.*,<sup>37</sup> and Kannan *et al.*<sup>38</sup> prepared methacrylate homopolymer with chalcone moiety, and crosslinked them by forming a cyclobutane ring after UV irradiation. Li *et al.* prepared a fluorinated chalcone-containing poly (arylene ether)<sup>39</sup> and poly(arylene ether sulfone).<sup>40</sup> They found that thermal properties and the Young's modulus increase after photo curing. Choi *et al.* prepared chalcone-containing epoxy.<sup>41</sup> They found that the cured chalcone-containing epoxy thermoset displayed a higher glass transition temperature and thermal stability than those of cured bisphenol epoxy without chalcone moiety.

To the best of our knowledge, no chalcone-containing benzoxazine has been reported in literature. Continuing other's and our effort in developing photo-sensitive benzoxazines,<sup>28–32</sup> we prepared a chalcone-containing benzoxazine, the 1,3-bis(4-hydroxyphenyl) propanone/aniline/formaldehyde-based benzoxazine (**BHP-a**,  $n = 0$  in Scheme 1) and evaluated the properties of its thermosets. Solubility test shows that the double bond of chalcone is thermally reactive. Therefore, two procedures were applied to cure **BHP-a**. The first one was thermal curing of the chalcone and oxazine moieties of **BHP-a**. The second one was photo curing of the chalcone moiety, followed by thermal curing of the oxazine moiety. Thermal properties of thermosets based on the two procedures were evaluated. Detailed syntheses and analysis are reported.

## Experimental

### Materials

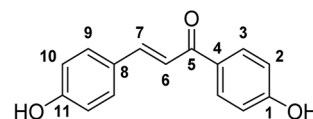
4-Hydroxybenzaldehyde (from Acros), 4-hydroxyacetophenone (from Alfa), and boron trifluoride diethyl etherate ( $\text{BF}_3 \cdot \text{OEt}_2$ , from Alfa), aniline (from Acros), paraformaldehyde (from Parac) and all solvents (HPLC grade) were purchased from various commercial sources and used without further purification.

### Characterization

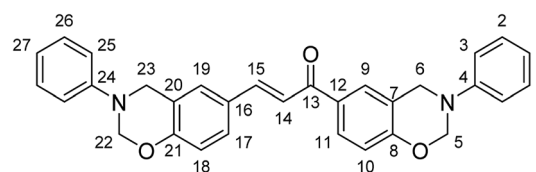
NMR measurements were performed using a Varian Inova 600 NMR in  $\text{DMSO}-d_6$ , and the chemical shift was calibrated by setting the chemical shift of  $\text{DMSO}-d_6$  at 2.49 ppm. Thermogravimetric analysis (TGA) was performed with a Perkin-Elmer Pyris1 at a heating rate of  $20^\circ\text{C min}^{-1}$  in an atmosphere of nitrogen or air. Differential scanning calorimetry (DSC) scans were obtained using a Perkin-Elmer DSC 7 in a nitrogen atmosphere at a heating rate of  $10^\circ\text{C min}^{-1}$ . Dynamic mechanical analysis (DMA) was performed using a Perkin-Elmer Pyris Diamond DMA with a sample size of  $5.0\text{ cm} \times 1.0\text{ cm} \times 0.2\text{ cm}$ . The storage modulus  $E'$  and  $\tan \delta$  were

determined as the sample was subjected to the temperature scan mode at a programmed heating rate of  $5^\circ\text{C min}^{-1}$  at a frequency of 1 Hz. The test was performed using a bending mode with an amplitude of  $5\text{ }\mu\text{m}$ . UV spectra were obtained using UV WinLab Lambda 25. IR spectra were obtained from at least 32 scans in the standard wavenumber range of  $667\text{--}4000\text{ cm}^{-1}$  using a Perkin-Elmer RX1 infrared spectrophotometer.

**Synthesis of 1,3-bis(4-hydroxyphenyl) propanone (BHP).** The chalcone-containing bisphenol, 1,3-bis(4-hydroxyphenyl) propanone (**BHP**) was prepared according to the procedure in literature.<sup>42</sup>  $^1\text{H-NMR}$  ( $\text{DMSO}-d_6$ ),  $\delta = 6.82$  (2H,  $\text{H}^{10}$ ), 6.89 (2H,  $\text{H}^2$ ), 7.61 (2H,  $\text{H}^6$ ), 7.67 (2H,  $\text{H}^7$ ), 7.69 (2H,  $\text{H}^9$ ), 8.03 (2H,  $\text{H}^3$ ), 10.02 (1H, OH), 10.34 (1H, OH).  $^{13}\text{C-NMR}$  ( $\text{DMSO}-d_6$ ),  $\delta = 115.30$  ( $\text{C}^{10}$ ), 115.78 ( $\text{C}^2$ ), 118.54 ( $\text{C}^7$ ), 125.99 ( $\text{C}^8$ ), 129.46 ( $\text{C}^4$ ), 130.72 ( $\text{C}^9$ ), 130.93 ( $\text{C}^3$ ), 143.16 ( $\text{C}^6$ ), 159.82 ( $\text{C}^{11}$ ), 161.90 ( $\text{C}^1$ ), 187.06 ( $\text{C}^5$ ). A melting peak at  $204^\circ\text{C}$  with an enthalpy of  $132\text{ J g}^{-1}$  was observed in the DSC thermogram. FT-IR (KBr):  $1601\text{ cm}^{-1}$  ( $\text{C}=\text{C}$  stretch),  $1648\text{ cm}^{-1}$  ( $\text{C}=\text{O}$  stretch),  $3325\text{ cm}^{-1}$  (OH stretch), UV-VIS  $\lambda_{\text{max}}$  ( $\text{C}_2\text{H}_5\text{OH}$ ) =  $351\text{ nm}$  ( $-\text{C}=\text{C}-$ ).



**Synthesis of 1,3-bis(4-hydroxyphenyl) propanone/aniline/formaldehyde-based benzoxazine (BHP-a).** **BHP** 10 g (0.042 mole), aniline 7.76 g (0.083 mole), paraformaldehyde 5.015 g (0.167 mmol) and xylene/1-butanol (2/1) 75 mL were introduced into a 250 mL round-bottom glass flask equipped with a condenser and a magnetic stirrer. The mixture was stirred at  $100^\circ\text{C}$  for 12 h. After cooling to room temperature, the precipitate was filtered and dried at  $70^\circ\text{C}$ . Yellow powder 8.58 g (43% yield) was obtained.  $^1\text{H-NMR}$  ( $\text{DMSO}-d_6$ ),  $\delta = 4.71$  (2H,  $\text{H}^{23}$ ), 4.78 (2H,  $\text{H}^6$ ), 5.53 (2H,  $\text{H}^{22}$ ), 5.58 (2H,  $\text{H}^5$ ), 6.79 (1H,  $\text{H}^{18}$ ), 6.87 (3H,  $\text{H}^1$ ,  $\text{H}^{10}$ ,  $\text{H}^{27}$ ), 7.15 (4H,  $\text{H}^3$ ,  $\text{H}^{25}$ ), 7.24 (4H,  $\text{H}^2$ ,  $\text{H}^{26}$ ), 7.61 (1H,  $\text{H}^{14}$ ), 7.62 (1H,  $\text{H}^{17}$ ), 7.67 (1H,  $\text{H}^{19}$ ), 7.74 (1H,  $\text{H}^{15}$ ), 7.92 (1H,  $\text{H}^{11}$ ), 8.02 (1H,  $\text{H}^9$ ).  $^{13}\text{C-NMR}$  ( $\text{DMSO}-d_6$ ),  $\delta = 48.77$  ( $\text{C}^{23}$ ), 48.82 ( $\text{C}^6$ ), 79.31 ( $\text{C}^{22}$ ), 79.56 ( $\text{C}^5$ ), 116.37 ( $\text{C}^{18}$ ), 116.72 ( $\text{C}^{10}$ ), 117.55 ( $\text{C}^3$ ,  $\text{C}^{25}$ ), 119.43 ( $\text{C}^{15}$ ), 120.78 ( $\text{C}^{27}$ ), 120.83 ( $\text{C}^1$ ), 121.28 ( $\text{C}^{20}$ ), 121.66 ( $\text{C}^7$ ), 127.25 ( $\text{C}^{16}$ ), 127.90 ( $\text{C}^{19}$ ), 128.41 ( $\text{C}^{11}$ ), 128.63 ( $\text{C}^9$ ), 128.83 ( $\text{C}^{17}$ ), 129.13 ( $\text{C}^2$ ,  $\text{C}^{26}$ ), 130.33 ( $\text{C}^{12}$ ), 143.02 ( $\text{C}^{14}$ ), 147.40 ( $\text{C}^{24}$ ), 147.54 ( $\text{C}^4$ ), 156.13 ( $\text{C}^{21}$ ), 158.16 ( $\text{C}^8$ ), 187.03 ( $\text{C}^{13}$ ). FTIR (KBr):  $934\text{ cm}^{-1}$  ( $\text{N}-\text{C}-\text{O}$  stretch),  $1032\text{ cm}^{-1}$  ( $\text{Ar}-\text{O}-\text{C}$  symmetric stretch),  $1232\text{ cm}^{-1}$  ( $\text{Ar}-\text{O}-\text{C}$  asymmetric stretch),  $1367\text{ cm}^{-1}$  ( $\text{C}-\text{N}$  stretch),  $1601\text{ cm}^{-1}$  ( $\text{C}=\text{C}$  stretch),  $1648\text{ cm}^{-1}$  ( $\text{C}=\text{O}$  stretch). A melting peak at  $159^\circ\text{C}$  with an enthalpy of  $41.8\text{ J g}^{-1}$ , and an exothermic peak at  $220^\circ\text{C}$  with an enthalpy of  $257\text{ J g}^{-1}$  were observed in the DSC thermogram.



## Sample preparation and curing procedure

**Preparation of P(BHP-a)-X.** P(BHP-a)-X is thermally curing thermoset of **BHP-a**. **BHP-a** was melted and stirred homogeneously on a hot plate, then cured at 180 °C (2 h) to obtain P(BHP-a)-180. A further curing at 200 °C (2 h) leads to P(BHP-a)-200. A further curing at 220 °C (2 h) leads to P(BHP-a)-220, and a further curing at 240 °C (2 h) results in P(BHP-a)-240.

**Preparation of P(BHP-a)-UV-X.** P(BHP-a)-UV-X is thermoset of **BHP-a** after photo-curing, followed by thermally curing. **BHP-a** was dissolved in DMAc to make a 20 wt% solution, and irradiated by UV (100 W, 365 nm) for 30 min. The solution was heated in an oven at 80 °C for 12 h to remove the solvent, then cured at 180 °C (2 h) to obtain P(BHP-a)-UV-180. A further curing at 200 °C (2 h) leads to P(BHP-a)-UV-200. A further curing at 220 °C (2 h) leads to P(BHP-a)-UV-220, and a further curing at 240 °C (2 h) results in P(BHP-a)-UV-240.

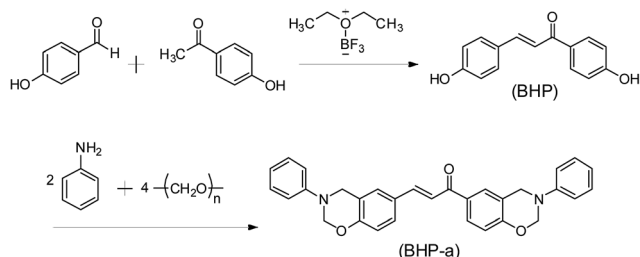
## Results and discussion

### Synthesis and characterization of BHP

In generally, a base such as sodium hydroxyl is traditionally used as a catalyst for the formation of chalcone moiety, but the yield and purity is not satisfied. Narender *et al.* reported that boron trifluoride diethyl etherate ( $\text{BF}_3 \cdot \text{OEt}_2$ ) lead to a faster reaction with better purity.<sup>33</sup> In this work, **BHP** was then prepared from 4-hydroxybenzaldehyde and 4-hydroxyacetophenone using  $\text{BF}_3 \cdot \text{OEt}_2$  as the catalyst (Scheme 2).<sup>42</sup> The characteristic peaks of  $\text{CH}=\text{CH}$  in **BHP** at 7.61 and 7.67 ppm, and the signal of phenolic OH at 10.02 and 10.34 ppm were observed in the  $^1\text{H}$ -NMR spectrum. The characteristic peaks of  $\text{CH}=\text{CH}$  in **BHP** at 143 and 118 ppm, and the signal of carbonyl at 187 ppm were observed in the  $^{13}\text{C}$ -NMR spectrum. Through the  $^1\text{H}$ - $^1\text{H}$  COSY and  $^1\text{H}$ - $^{13}\text{C}$  HERCOR (Fig. S1 and S2<sup>†</sup>), the signals of aromatic hydrogen (H2, H3, H9, and H10) and aromatic carbons (C1–C4, C8–C11) can be correctly assigned. A sharp melting point at 204 °C with an enthalpy of 132 J g<sup>−1</sup> was observed in the DSC thermogram. Analytic data show that **BHP** was successfully prepared.

### Synthesis and characterization of benzoxazine (BHP-a)

**BHP-a** was prepared by Mannich condensation of (**BHP**), aniline and formaldehyde (Scheme 2). Fig. 1 shows the  $^1\text{H}$ -NMR spectra of the reaction product prepared in different reaction media.



Scheme 2 Synthesis of 1,3-bis(4-hydroxyphenyl) propanone (**BHP**) and **BHP**/aniline/formaldehyde-based benzoxazine (**BHP-a**).

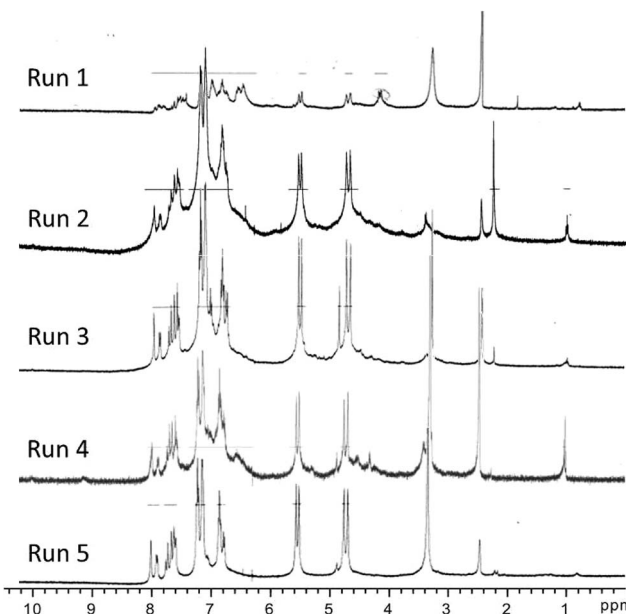


Fig. 1  $^1\text{H}$ -NMR spectra of reaction product prepared in different reaction media. Run 1, 80 °C/12 h in 1,4-dioxane; Run 2, 80 °C/12 h in toluene/ethanol (V/V = 2/1); Run 3, 80 °C/12 h in toluene/ethanol (V/V = 1/1); Run 4, 80 °C/12 h in toluene/ethanol (V/V = 1/2); Run 5, 100 °C/12 h in xylene/1-butanol (V/V = 2/1).

The effect of reaction media on the purity of **BHP-a** is discussed. Reacting in 1,4-dioxane (Run 1), a common solvent for Mannich condensation, at 80 °C for 12 h leads to low conversion and byproducts. Using toluene/ethanol as solvents (volume ratio 2/1, 1/1, and 1/2 for Runs 2–4) at 80 °C for 12 h leads to better conversion, but the ratio of the integral area to Ar-H/oxazine is far from the theoretical ratio of 4.5. The co-solvent of toluene/ethanol was a recommended medium for Mannich condensation in our previous work for benzoxazine synthesis.<sup>43</sup> Thus, we thought that an incomplete reaction was due to the electron-withdrawing carbonyl group of **BHP** that reduces the reactivity of phenolic OH. To increase the reaction rate, a co-solvent for a higher temperature reaction was applied. The co-solvent was changed to xylene/1-butanol (V/V = 2/1), and reacting at 100 °C for 12 h (Run 5). As expected, the NMR spectrum shows that increasing the reaction temperature lead to **BHP-a** with a higher yield and purity (detailed NMR analysis will be discussed in Fig. 2).

Fig. 2 shows the (a)  $^1\text{H}$ -NMR and (b)  $^{13}\text{C}$ -NMR spectra of **BHP-a**. Since the two oxazine linkage in **BHP-a** was asymmetrical, the oxazine signals split slightly due to the different chemical environment. In Fig. 2a, the characteristic peaks of oxazine at 4.71 and 4.78 ppm ( $\text{H}^{23}$  and  $\text{H}^6$ ), 5.53 and 5.58 ppm ( $\text{H}^{22}$  and  $\text{H}^5$ ) were clearly observed. In addition, no signal of phenolic OH was observed, suggesting that the Mannich condensation was complete. In Fig. 2b, the characteristic peaks of oxazine at 48.77 and 48.82 ppm ( $\text{C}^{23}$  and  $\text{C}^6$ ), 79.31 and 79.56 ppm ( $\text{C}^{22}$  and  $\text{C}^5$ ) were observed. Through  $^1\text{H}$ - $^1\text{H}$  COSY (Fig. S3<sup>†</sup>) and  $^1\text{H}$ - $^{13}\text{C}$  HERCOR (Fig. S4<sup>†</sup>), the signals of aromatic hydrogen and aromatic carbons were correctly assigned. Fig. 3 shows the DSC heating thermogram of **BHP-a**. A sharp melting point at 159 °C



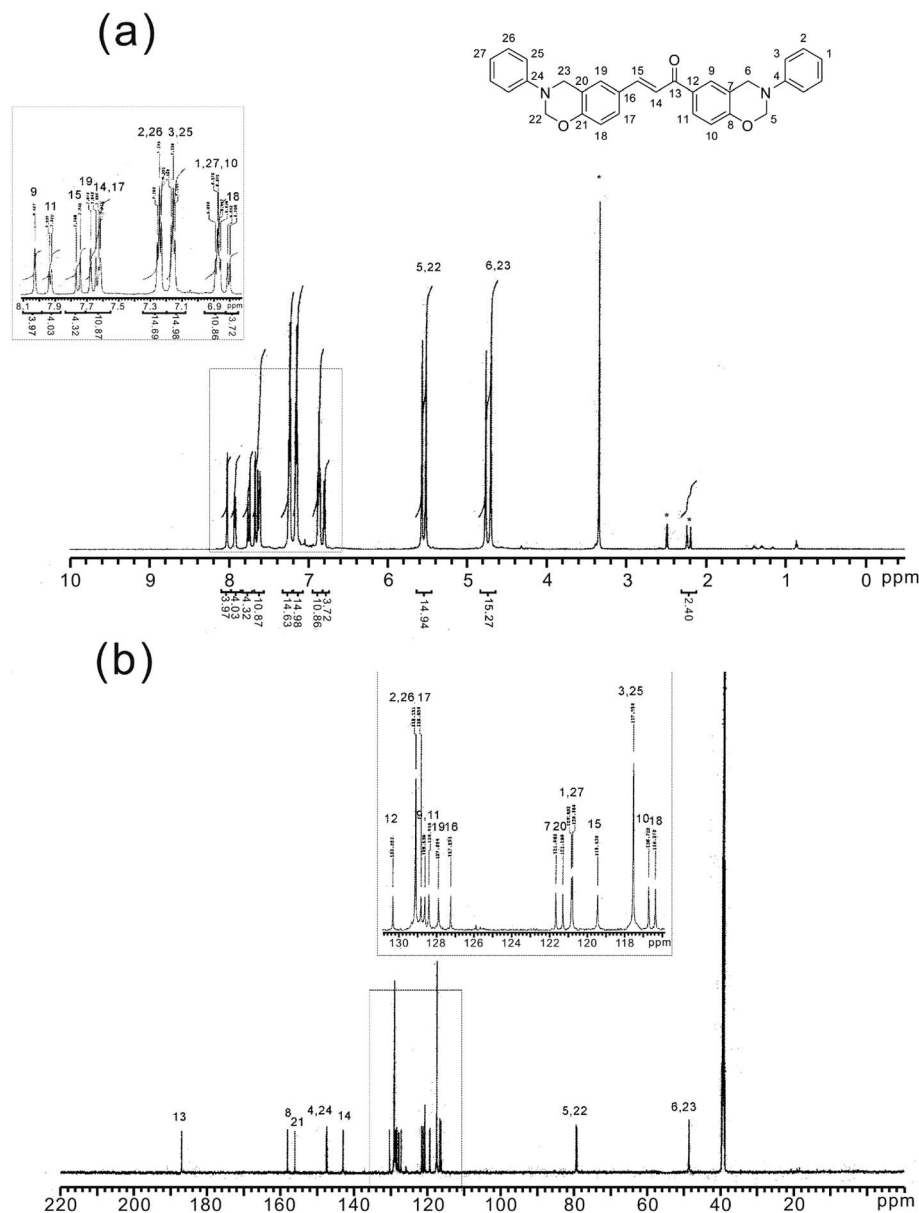


Fig. 2 (a)  $^1\text{H}$  NMR and (b)  $^{13}\text{C}$  NMR spectra of BHP-a in  $\text{DMSO}-d_6$ .

with an  $\Delta H$  of  $41 \text{ J g}^{-1}$ , followed by an exothermic peak at  $220^\circ\text{C}$  with  $\Delta H$  of  $257 \text{ J g}^{-1}$  were observed. The sharp melting point demonstrates the purity of BHP-a. Since the melting point and exothermic peak temperature of BHP-a are  $159$  and  $220^\circ\text{C}$ , respectively, the processing window is about  $60^\circ\text{C}$ .

#### Thermal properties of thermally-cured poly(BHP-a)

Fig. S5† shows a photo of BHP in DMSO after thermal treatment at various temperatures for 20 min. BHP is soluble in DMSO until it is thermally treated at a temperature higher than  $240^\circ\text{C}$ , suggesting that a crosslinking structure is formed. It is known that photo-crosslinking of chalcone leads to a dimer with a cyclobutane structure. However, dimerization will not lead to

a crosslinking structure. This result indicates that the double bond of chalcone, like general vinyl compounds, can be polymerized through thermal treatment. Therefore, there are two thermally curable moieties in BHP-a. The first one is the double bond of chalcone (marked in red in Scheme 3), and the second one is benzoxazine (marked in blue in Scheme 3). Fig. 4 shows DMA thermograms of the thermosets for BHP-a, the P(BHP-a)-X, in which X is the final curing temperature.  $T_g$  values taken from the peak temperature of  $\tan \delta$  are  $254$ ,  $263$ ,  $268$ , and  $294^\circ\text{C}$  for X as  $180$ ,  $200$ ,  $220$  and  $240$ , respectively (Table 1). The peak intensity (height) of  $\tan \delta$  decreases gradually with the curing temperature, suggesting that the rigidity increases with the increase in curing temperature. The  $T_g$  values of the P(BHP-a)-X and P(BHBA-a)-X<sup>32</sup> were plotted in Fig. 8a. The difference





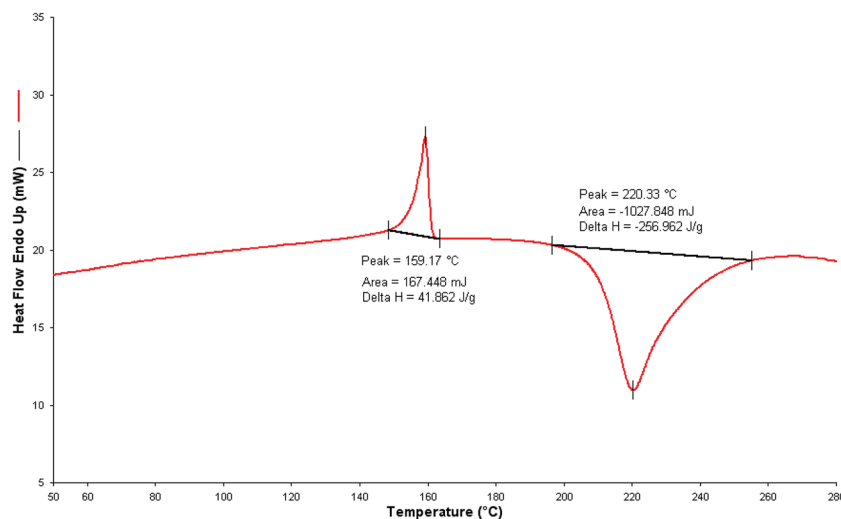
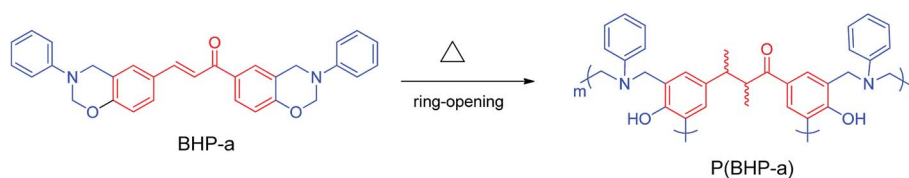


Fig. 3 DSC thermogram of BHP-a.



Scheme 3 Thermally curing of BHP-a.

between P(BHBA-a)-220 and P(BHP-a)-220 was 8 °C, and was 24 °C between P(BHBA-a)-240 and P(BHP-a)-240. We think that BHBA-a has one more unsaturated double bond than BHP-a, leading to a higher crosslinking density, and thus a higher  $T_g$ . Although the  $T_g$  value (294 °C) of P(BHP-a)-240 is slightly lower than that (318 °C) of P(BHBA-a)-240,<sup>32</sup> the value of 294 °C is much higher than that (around 150–160 °C) of a thermoset of bisphenol-based benzoxazines such as bisphenol A/aniline-based poly(B-a), and bisphenol F/aniline-based poly(F-a).<sup>1,2</sup>

The high  $T_g$  value supports the crosslinking of the double bond of chalcone in BHP-a. Table 1 lists the thermal stability data of P(BHP)-X. Thermal stability increases with the increase in curing temperature, probably due to the increasing degree of curing. P(BHP-a)-240 has a 5 wt% decomposition temperature at 431 °C in nitrogen atmosphere, and 435 °C in air atmosphere, and with a char yield at 800 °C is as high as 68% in nitrogen atmosphere. Generally, thermosets of bisphenol-based

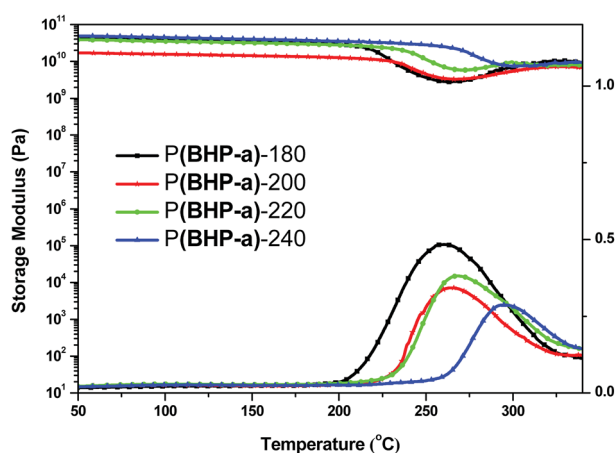


Fig. 4 DMA thermograms of P(BHP-a)-X.

Table 1 Thermal properties of P(BHP-a)-X and P(BHP-a)-UV-X

Sample ID	tan $\delta$ (°C) (DMA) <sup>a</sup>	$T_{d5\%}$ <sup>b</sup> (°C)		Char yield <sup>c</sup> (%)	
		N <sub>2</sub>	air	N <sub>2</sub>	air
P(BHP-a)-180	254	—	—	—	—
P(BHP-a)-200	263	395	408	67	0
P(BHP-a)-220	268	414	412	67	0
P(BHP-a)-240	294	431	435	68	0
P(BHP-a)-UV-180	273	—	—	—	—
P(BHP-a)-UV-200	296	335	349	58	0
P(BHP-a)-UV-220	313	373	379	62	0
P(BHP-a)-UV-240	328	378	392	P60	0

<sup>a</sup> Measured by DMA at a heating rate of 5 °C min<sup>-1</sup>;  $T_g$  were determined from a peak temperature of the tan  $\delta$  curve. <sup>b</sup> Temperature corresponding to 5% weight loss by thermogravimetry at a heating rate of 20 °C min<sup>-1</sup> in nitrogen and air. <sup>c</sup> Residual weight% at 800 °C in nitrogen and air.



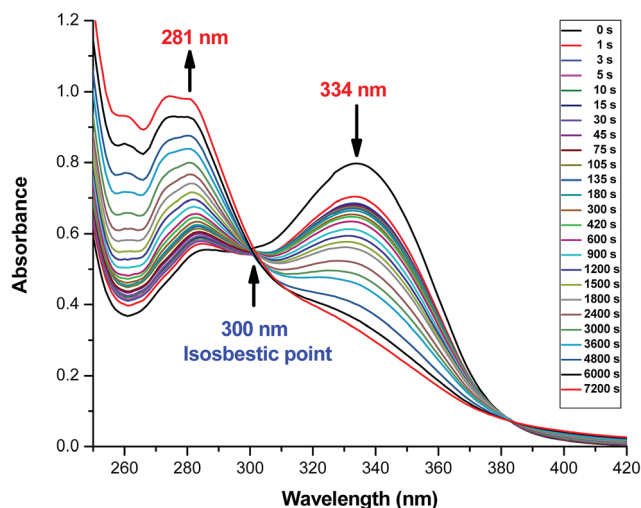


Fig. 5 UV absorption spectra of BHP-a in DMAc ( $10^{-2}$  M) after irradiating at 365 nm for various periods of time.

benzoxazines such as bisphenol A/aniline-based, and bisphenol F/aniline-based benzoxazine exhibit 5 wt% decomposition temperature at around 300–350 °C.<sup>1,2</sup> The high decomposition temperature of P(BHP-a) is impressive.

#### Thermal properties of UV and thermally-cured poly(BHP-a)

Fig. 5 shows the UV absorption spectra of BHP-a in DMAc ( $10^{-2}$  M) after irradiating at 365 nm for various periods of time. An isosbestic point at 300 nm, a  $\pi$ - $\pi^*$  absorption of a double bond of chalcone at 334 nm, and a  $\delta$ - $\delta^*$  absorption of cyclobutane at 281 nm were observed. The intensity of the  $\pi$ - $\pi^*$  absorption decreases with the irradiation time, and the  $\delta$ - $\delta^*$  absorption increases with the irradiation time. The UV absorption data indicate the formation of a BHP-a dimer, as shown in Scheme 4.

Fig. 6 shows the  $^1\text{H}$ -NMR spectra of BHP-a after irradiating at 365 nm for various periods of time. Two new absorptions at 4.6 and 5.4 ppm corresponding to the cyclobutane structure in BHP-a dimer appear after irradiating for 5 min. This new absorption of cyclobutane is consistent with that of the UV analysis (Fig. 6). The signals for oxazine at 4.7 and 5.6 ppm are

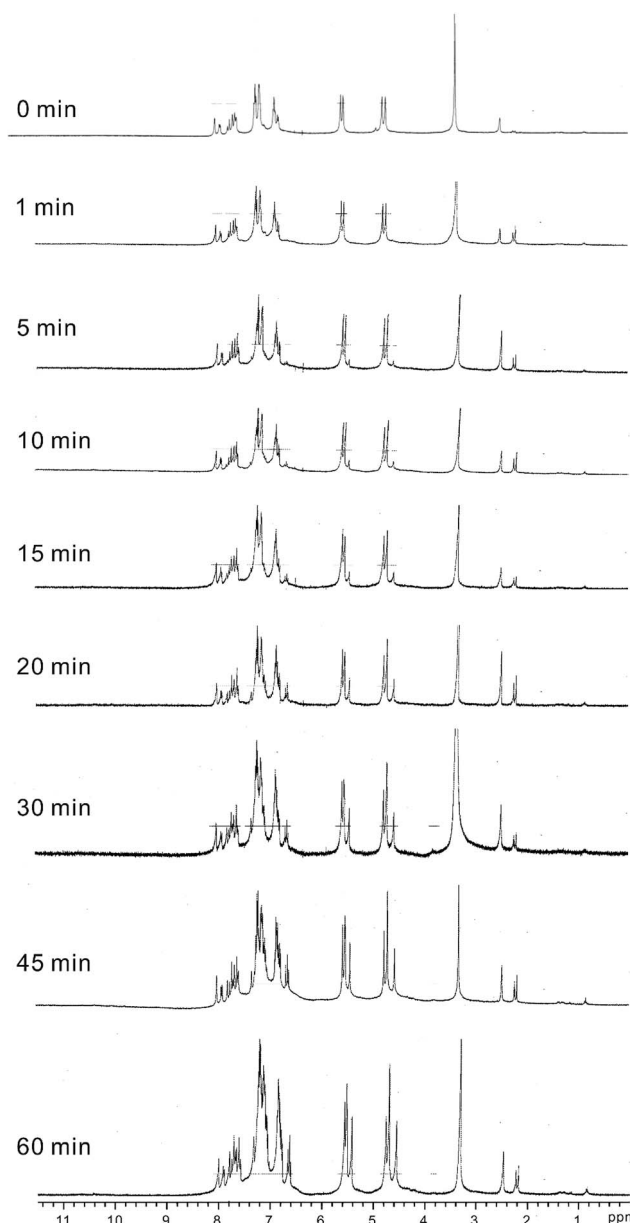
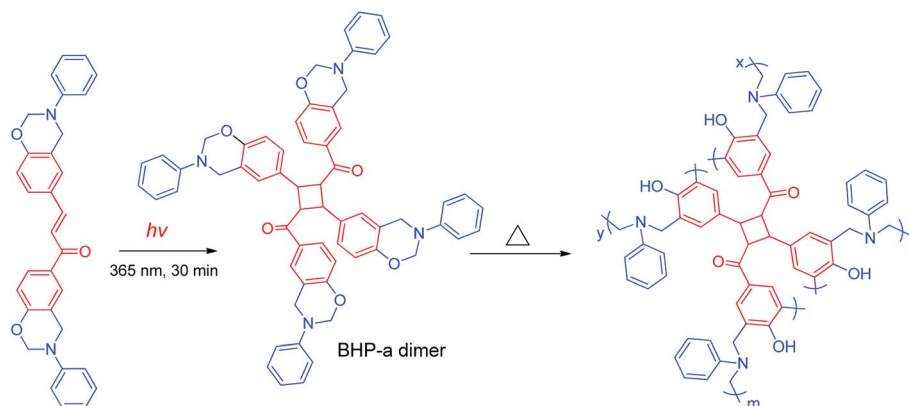


Fig. 6  $^1\text{H}$ -NMR spectra of BHP-a after irradiating at 365 nm for various periods of time.



Scheme 4 Photo-curing of BHP-a, followed by thermally curing BHP-a dimer.



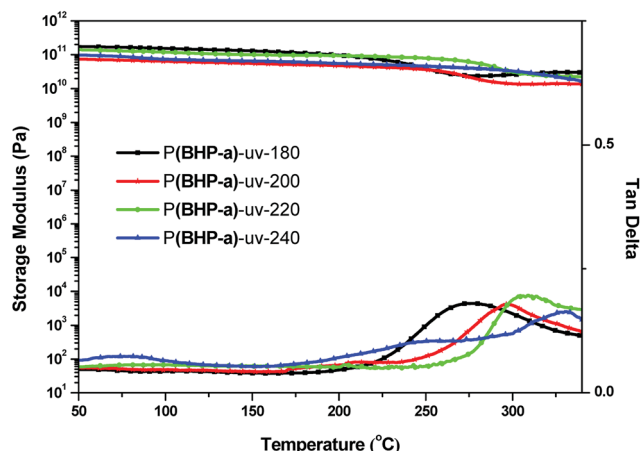


Fig. 7 DMA thermograms of P(BHP-a)-UV-X.

intact open UV irradiation, suggesting that the oxazine is stable under the UV irradiation we have applied. Scheme 4 shows the photo-curing of **BHP-a**, followed by thermally curing. The oxazines of **BHP-a** dimer can be thermally-cured, leading to P(**BHP-a**)-UV-X.

Fig. 7 shows DMA thermograms of P(**BHP-a**)-UV-X, in which X is the final curing temperature.  $T_g$  values taken from the peak temperature of  $\tan \delta$  are 273, 296, 313, and 328 °C for X as 180, 200, 220, and 240, respectively. The  $T_g$  value of P(**BHP-a**)-UV-X is higher than that of P(**BHP-a**)-X, indicating that the **BHP-a** dimer, a tetra-functional benzoxazine, contributes to a higher crosslinking density.<sup>29</sup> The peak intensity (height) of  $\tan(\delta)$  in Fig. 7 is much less than that in Fig. 4, further demonstrating a higher crosslinking density for P(**BHP-a**)-UV-X. The  $T_g$  values of the P(**BHP-a**)-UV-X and P(**BHBA-a**)-UV-X<sup>32</sup> were plotted in Fig. 8b. The difference between P(**BHBA-a**)-UV-220 and P(**BHP-a**)-UV-220 was 5 °C, and was 14 °C between P(**BHBA-a**)-UV-240 and P(**BHP-a**)-UV-240. We speculate the one more unsaturated double bond in **BHBA-a** dimer than **BHP-a** dimer,<sup>32</sup> leading to a higher crosslinking density at high curing temperature. Therefore, the gap increase slightly with the curing temperature. TGA thermogram shows that the 5 wt% decomposition

temperature of P(**BHP-a**)-UV-240 is 378 °C in a nitrogen atmosphere, and 392 °C in an air atmosphere, and with char yield at 800 °C in nitrogen atmosphere as high as 60% in nitrogen atmosphere. The thermal stability of P(**BHP-a**)-UV-X is slightly lower than P(**BHP-a**)-X, probably due to the less thermal stability of cyclobutane moiety or the degradation of polymer chains during UV irradiation.

## Conclusions

We have successfully prepared a bifunctional chalcone-containing benzoxazine (**BHP-a**) from 1,3-bis(4-hydroxyphenyl) propanone (**BHP**), aniline and paraformaldehyde in a co-solvent of xylene/1-butanol (V/V = 2/1) (Fig. 1). The double bond of chalcone is thermally reactive, as evidenced by the insolubility of **BHP** after thermal treatment at temperatures 240 °C for 20 min (Fig. S5†). The chalcone moiety can be photo-cured to afford a tetrafunctional benzoxazine, **BHP-a** dimer, as supported by the UV absorption (Fig. 5) and <sup>1</sup>H-NMR (Fig. 6) spectra. Therefore, two curing procedures were applied for **BHP-a** to afford the thermosets. The first one was thermal curing of the chalcone and oxazine moieties, forming thermosets P(**BHP-a**)-X. The second one was photo-curing of the chalcone moiety, followed by thermally curing of the oxazine moiety, forming thermosets P(**BHP-a**)-UV-X. P(**BHP-a**)-240 exhibit a  $T_g$  value as high as 294 °C, according to the DMA thermogram (Fig. 4). The crosslinking of the double bond of chalcone, as shown in Scheme 3, might be responsible for  $T_g$  being much higher than that for general poly-benzoxazines without chalcone moiety. According to the DMA thermogram (Fig. 7), P(**BHP-a**)-UV-240 exhibits a  $T_g$  value as high as 328 °C. The  $T_g$  value of P(**BHP-a**)-UV-X is higher than that of P(**BHP-a**)-X, indicating that the **BHP-a** dimer, a tetra-functional benzoxazine, contributes to a higher crosslinking density. Although the  $T_g$  value of P(**BHP-a**)-X is slightly lower than that of P(**BHBA-a**)-X,<sup>32</sup> probably due to **BHBA-a** has one more unsaturated double bond than **BHP-a**, leading to a higher crosslinking density. However, the difference is small. Therefore, incorporating chalcone into benzoxazine appears to be a alternative strategy to afford high-performance benzoxazine thermosets.

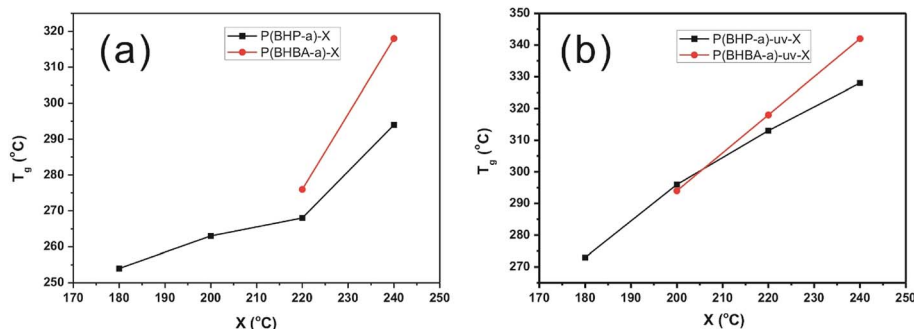


Fig. 8  $T_g$  values of (a) P(**BHP-a**)-X and P(**BHBA-a**)-X<sup>32</sup> (b) P(**BHP-a**)-UV-X and P(**BHBA-a**)-UV-X.<sup>32</sup>



## Acknowledgements

Financial support of this work from the Ministry of Science and Technology (MOST 104-2628-E-005-002-MY3), Taiwan is highly appreciated.

## Notes and references

- 1 X. Ning and H. Ishida, *J. Polym. Sci., Part A: Polym. Chem.*, 1994, **32**, 1121–1129.
- 2 J. Liu and H. Ishida, *Macromolecules*, 2014, **47**, 5682–5690.
- 3 Y. Yagci, B. Kiskan and N. N. Ghosh, *J. Polym. Sci., Part A: Polym. Chem.*, 2009, **47**, 5565–5576.
- 4 N. N. Ghosh, B. Kiskan and Y. Yagci, *Prog. Polym. Sci.*, 2007, **32**, 1344–1391.
- 5 S. N. Kolanadiyil and T. Endo, *Macromolecules*, 2016, **49**, 8466–8478.
- 6 C. Rodriguez Arza, P. Froimowicz and H. Ishida, *RSC Adv.*, 2015, **5**, 97855–97861.
- 7 A. W. Kawaguchi, A. Sudo and T. Endo, *J. Polym. Sci., Part A: Polym. Chem.*, 2014, **52**, 410–416.
- 8 M. Arslan, B. Kiskan and Y. Yagci, *Macromolecules*, 2015, **48**, 1329–1334.
- 9 S. Zhang, P. Yang, Y. Bai, T. Zhou, R. Zhu and Y. Gu, *ACS Omega*, 2017, **2**, 1529–1534.
- 10 S. Li and S. Yan, *RSC Adv.*, 2015, **5**, 61808–61814.
- 11 L. Zhang, Y. Zhu, D. Li, M. Wang, H. Chen and J. Wu, *RSC Adv.*, 2015, **5**, 96879–96887.
- 12 P. Thirukumaran, A. Shakila and S. Muthusamy, *RSC Adv.*, 2014, **4**, 7959–7966.
- 13 Y. Xu, Q. Ran, C. Li, R. Zhu and Y. Gu, *RSC Adv.*, 2015, **5**, 82429–82437.
- 14 K. Zhang, Q. Zhuang, X. Liu, R. Cai, G. Yang and Z. Han, *RSC Adv.*, 2013, **3**, 5261–5270.
- 15 S.-K. Kim, S.-W. Choi, W. S. Jeon, J. O. Park, T. Ko, H. Chang and J.-C. Lee, *Macromolecules*, 2012, **45**, 1438–1446.
- 16 H. Ishida and D. J. Allen, *J. Polym. Sci., Part B: Polym. Phys.*, 1996, **34**, 1019–1030.
- 17 C. F. Wang, Y. C. Su, S. W. Kuo, C. F. Huang, Y. C. Sheen and F. C. Chang, *Angew. Chem., Int. Ed.*, 2006, **45**, 2248–2251.
- 18 H. Wang, R. Zhu, P. Yang and Y. Gu, *Polym. Chem.*, 2016, **7**, 860–866.
- 19 R. Kudoh, A. Sudo and T. Endo, *Macromolecules*, 2010, **43**, 1185–1187.
- 20 H. Oie, A. Sudo and T. Endo, *J. Polym. Sci., Part A: Polym. Chem.*, 2010, **48**, 5357–5363.
- 21 H. Oie, A. Mori, A. Sudo and T. Endo, *J. Polym. Sci., Part A: Polym. Chem.*, 2012, **50**, 4756–4761.
- 22 S. Shukla and B. Lochab, *Polymer*, 2016, **99**, 684–694.
- 23 H. Wang, J. Wang, X. He, T. Feng, N. Ramdani, M. Luan, W. Liu and X. Xu, *RSC Adv.*, 2014, **4**, 64798–64801.
- 24 T. Zhang, J. Wang, T. Feng, H. Wang, N. Ramdani, M. Derradji, X. Xu, W. Liu and T. Tang, *RSC Adv.*, 2015, **5**, 33623–33631.
- 25 J. Wang, W. Liu and T. Feng, in *Advanced and Emerging Polybenzoxazine Science and Technology*, ed. P. Froimowicz, Elsevier, Amsterdam, 2017, pp. 533–567, DOI: 10.1016/b978-0-12-804170-3.00028-7.
- 26 L. Jin, T. Agag, Y. Yagci and H. Ishida, *Macromolecules*, 2011, **44**, 767–772.
- 27 B. Koz, B. Kiskan and Y. Yagci, *Polym. Bull.*, 2011, **66**, 165–174.
- 28 B. Kiskan and Y. Yagci, *J. Polym. Sci., Part A: Polym. Chem.*, 2007, **45**, 1670–1676.
- 29 M. G. Mohamed, K.-C. Hsu and S.-W. Kuo, *Polym. Chem.*, 2015, **6**, 2423–2433.
- 30 R.-C. Lin, M. G. Mohamed, K.-C. Hsu, J.-Y. Wu, Y.-R. Jheng and S.-W. Kuo, *RSC Adv.*, 2016, **6**, 10683–10696.
- 31 B. Kiskan and Y. Yagci, *J. Polym. Sci., Part A: Polym. Chem.*, 2014, **52**, 2911–2918.
- 32 C. H. Lin, Z. J. Chen, C. H. Chen, M. W. Wang and T. Y. Juang, *ACS Omega*, 2017, **2**, 3432–3440.
- 33 T. Narender and K. Papi Reddy, *Tetrahedron Lett.*, 2007, **48**, 3177–3180.
- 34 K. Feng, M. Tsushima, T. Matsumoto and T. Kurosaki, *J. Polym. Sci., Part A: Polym. Chem.*, 1998, **36**, 685–693.
- 35 D.-m. Song, K.-h. Jung, J.-h. Moon and D.-m. Shin, *Opt. Mater.*, 2003, **21**, 667–671.
- 36 A. Rehab and N. Salahuddin, *Polymer*, 1999, **40**, 2197–2207.
- 37 R. Balaji and S. Nanjundan, *React. Funct. Polym.*, 2001, **49**, 77–86.
- 38 S. Balamurugan, S. Nithyanandan, C. Selvarasu, G. Y. Yeap and P. Kannan, *Polymer*, 2012, **53**, 4104–4111.
- 39 W. Tie, Z. Zhong, P. Wen, M.-H. Lee and X.-D. Li, *Mater. Lett.*, 2009, **63**, 1381–1383.
- 40 W. Tie, Z. Zhong, L. Li, A. Zhang, F. Shen, M.-H. Lee and X.-D. Li, *Eur. Polym. J.*, 2012, **48**, 2070–2075.
- 41 D. H. Choi, S. J. Oh, H. B. Cha and J. Y. Lee, *Eur. Polym. J.*, 2001, **37**, 1951–1959.
- 42 K. Kaniappan and S. Murugavel, *J. Appl. Polym. Sci.*, 2009, **111**, 1606–1614.
- 43 C. H. Lin, S. L. Chang, T. Y. Shen, Y. S. Shih, H. T. Lin and C. F. Wang, *Polym. Chem.*, 2012, **3**, 935–945.

